Journal of Applied Polymer Science

Enhancement in the Thermal and Dynamic Mechanical Properties of High Performance Liquid Crystalline Epoxy Composites Through Uniaxial Orientation of Mesogenic on Carbon Fiber

Huilong Guo,[1,2] Mangeng Lu,[1] Liyan Liang,[1] Jian Zheng,[1,2] Yunfei Zhang,[1,2] Yinwen Li,[1,2] Zhaoxia Li,[1,2] Chenghua Yang[1,2]

[1]Guangzhou Institute of Chemistry, Chinese Academy of Sciences, Guangzhou 510650, People's Republic of China
[2]University of Chinese Academy of Sciences, Beijing 100049, People's Republic of China
Correspondence to: M. Lu (E-mail: mglu@gic.ac.cn)

ABSTRACT: In this work, a high performance liquid crystalline epoxy composite was prepared and the effect of the alignment of LCE with long lateral substituent on the carbon fiber surface curing at low temperature on fracture toughness, dynamic mechanical, and thermal properties of liquid crystalline epoxy with lateral substituent (LCE6) was investigated by polarized optical microscopy (POM), wide angle X-ray diffraction measurements (WAXS), dynamic mechanical analysis (DMA), thermogravimetric (TGA), and scanning electron microscopy (SEM). Curing degree of the composite was observed by FTIR. The experimental results indicate that the fracture toughness, glass transition temperature (T_g), thermal stability, degradation kinetics are associated with the alignment of LCE6 along long axis of carbon fiber. The alignment of LCE6 on carbon fiber surface can increase mesogen network density, which leads to higher fracture toughness, higher thermal stability, increase of the activation energies and higher T_g of the composite. The dynamic mechanical analysis shows that the compoaite possesses extremely higher dynamic storage moduli, which indicates that this LCE6/DDM/CF composite can be a high performance composite. Thus, the compoaite can be a potential candidate for advanced composites. © 2014 Wiley Periodicals, Inc. J. Appl. Polym. Sci. **2014**, *131*, 40363.

KEYWORDS: fibers; liquid crystals; thermal properties; mechanical properties; morphology

Received 9 October 2013; accepted 30 December 2013
DOI: 10.1002/app.40363

INTRODUCTION

Liquid crystalline epoxides (LCEs) have so many desirable characteristics, such as good mechanical and dielectric properties in the direction of orientation, very good dimensional stability, tuned coefficients of thermal expansion, increased fracture toughness, and noticeable high temperature properties, that these epoxides can be applied into aerospace structural materials and other high performance devices.[1,2] Therefore, LCEs are especially suitable for being used as advanced composites matrix.[3]

Carbon fibers (CF) possess high tensile (HT) strength up to 7 GPa with excellent creep resistance, low densities (ρ =1.75–2.00 g/cm^3) and high moduli (HM) up to 900 Gpa, which make carbon fiber attractive for application in advanced composites.[4]

Mally et al. prepared a carbon-fiber/epoxy composite and detailed the test and performance of the composite for the underwater repair of pressure equipment.[5] Carfagna et al. reported the application of carbon fiber advanced composites with LCE resins used as matrix materials and indicated an increased mechanical performances, a good adhesion between LCE resins and carbon fiber and that this new material is of great potential for advanced composites.[6–8] Lee et al. investigated anisotropic orientation of LCE resin and transverse alignment of LCE resin on carbon fiber surface.[9,10] However, no report has been published concerning the effect of the alignment of LCE6 along long carbon fiber axis curing at low temperature on dynamic mechanical properties, fracture toughness, and thermal properties of liquid crystalline epoxy. It was reported by Marta Giamberini et al. that a kinetic analysis of TGA data demonstrated LC system possesses a higher activation energy compared to isotropic (ISO) system.[11] Mallon et al. confirmed that liquid crystal could be aligned on carbon fiber surface.[12,13] It was also reported by Lee et al. that LCE resin was aligned along the long molecular axis of carbon fiber at low curing temperature.[9] Therefore, it was expected that anisotropically aligned network, which was formed by LCE6 aligning along the long molecular axis of carbon fiber at low curing temperature, could improve dynamic mechanical properties, toughness, and thermal properties of liquid crystalline epoxy. And

this composite could be especially suitable for aerospace structural applications.

This article deals with the preparation and characterization of a composite based on carbon fiber and LCE with long lateral substituent. In this study, the alignment of LCE with long lateral substituent on the carbon fiber surface curing at low temperature was investigated through a polarized optical microscope and wide angle X-ray diffraction measurements. The fracture surface was observed by SEM. DSC was performed to characterize the glass transition temperature (T_g). TGA was used to investigate effect of carbon fiber on thermal stability of liquid crystalline epoxy with long lateral substituent and TGA data obtained at different heating rate was also carried out to study the degradation kinetics. DMA was used to analyze the storage moduli (E'), loss moduli (E''), and loss tangent (tan δ). In addition, the curing degree was investigated through FTIR spectrum.

EXPERIMENTAL

Materials

LCE with lateral substituent (LCE6) (2,5 - bis [4-(glycidyl ether) benzoyloxy] benzoic acid n-hexyl ester, see Figure 1) was synthesized in our laboratory according to the program proposed by our group in early reports.[14,15] The mechanical properties, including tensile strength, Young's modulus and elongation at break, decrease as increase of the length of lateral substituent. Larger substituents lead to decreased cross-linking densities of the LC networks.[16,17] Therefore, we synthesized LCE6 as matrix of the composites, for the better comprehensive performance of LCE6 like better toughness than LCE2 and LCE4, better mechanical properties than LCE8, LCE10 and LCE12. DDM (see Figure 1) was purchased from Aladdin and was used as curing agent. Carbon fabric (300 g/m^2 plain, UT70-30C) was purchased from Toray Industries (China) and was cleaned in dichloro-methane for 3 days, distilled water for 1 day and dried in vacuum at 100°C for 2 days before using.

Composites Manufacturing

The stoichiometric amount of LCE6 and DDM was dissolved in dichloromethane, a layer of carbon fabric was infiltrated by the mixed solution of LCE6/DDM in the refrigerator for 24 h. Then dichloromethane was removed under reduced pressure at room temperature, the percentage of carbon fibers with respect to the matrix was 33 wt %. The samples were curied at low temperature of 75°C which is the isotropic temperature of LCE6/DDM mixtures, for 16 h to ensure the totally reaction of linear chain extension and postcured at 160°C for 6 h, 200°C for 1 h to guarantee completely branching and crosslinking. After curing, the cured product were extracted from the mold, to be tested. LCE6/DDM resin was manufactured through the same curing process, in order to be compared with the composites.

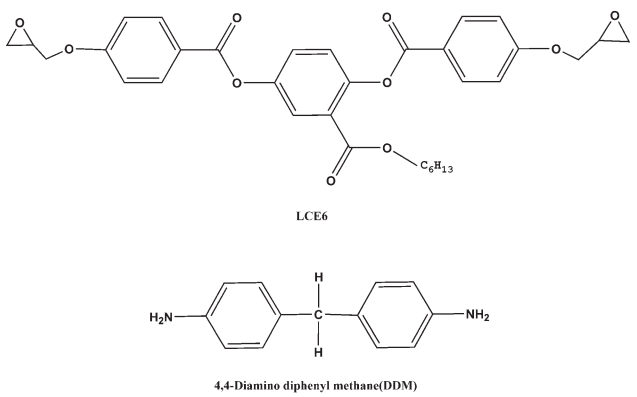

Figure 1. Chemical structures of LCE6 and DDM.

Physical Measurements

The alignment of LCE with long lateral substituent on the carbon fiber surface was examined by an polarized light optical microscopy (POM) (Orthoglan, LEITZ, Germany) and wide angle X-ray diffraction measurements (WAXS) which were carried out with a Rigaku Diffractometer (D/MAX-1200), using monochromatic Cu Karadiation (40 kV, 30 mA) and secondary graphite monochromator, with the X-ray scatting intensities being detected by a scintillation counter incorporating a pulse-height analyzer.

The morphology of the fracture surface after tensile tests was observed using a Philips XL30 scanning electron microscope (SEM).

Infrared spectra, recorded on a WQF-410 Fourier Transform Infrared (FTIR) spectrometer, was used to investigate the change of epoxy ring before and after curing.

The response of the samples to small-strain mechanical deformation was measured as a function of temperature (−120 to 200°C) using a NETZSCH DMA 242 dynamic mechanical analyzer in a DualCantilever2x16 stress mode. The testing was carried out at a heating rate of 5°C/min in a N_2 atmosphere, frequencies of 1 Hz and 2 Hz, a dynamic stress of 5 N, and a static stress of 0.5 N. The sample displacement was 30 μm. Storage moduli (E'), loss moduli (E''), and loss tangent (tan δ) were recorded.

The effect of carbon fiber on thermal stability of liquid crystalline epoxy with long lateral substituent was carried out by thermogravimetrical analysis (TGA) (Pyris 1 TGA, PE) instrument in flowing nitrogen (20 mL/min) at a heating rate 10°C/min from 40 to 800°C. And the degradation kinetics was studied by TGA data obtained at different heating rate (5°C/min, 10°C/min, 20°C/min) from 40 to 800°C.

RESULTS AND DISCUSSION

The Alignment of LCE6 on Carbon Fiber Surface

Figure 2 shows the polarized optical microscopic pictures during curing of LCE6/DDM (a–f) and LCE6/DDM/CF (g–l). Comparing POM of LCE6/DDM and LCE6/DDM/CF, both show common nematic structure at 25°C, CF does not effect the nematic structure. At the beginning of temperature jump to 75°C, the mixtures start to loss property of birefringence and exhibit homogeneity until 5 minutes. Then during curing the alignment of LCE6 along carbon fiber long axis emerge in the composites, while in LCE6/DDM mixtures only common nematic structure can be seen. Subsequently, POM of LCE6/DDM/CF composites after postcuring cooling down to room temperature illustrate a more regular uniaxially oriented nematic structure along carbon fiber long axis.

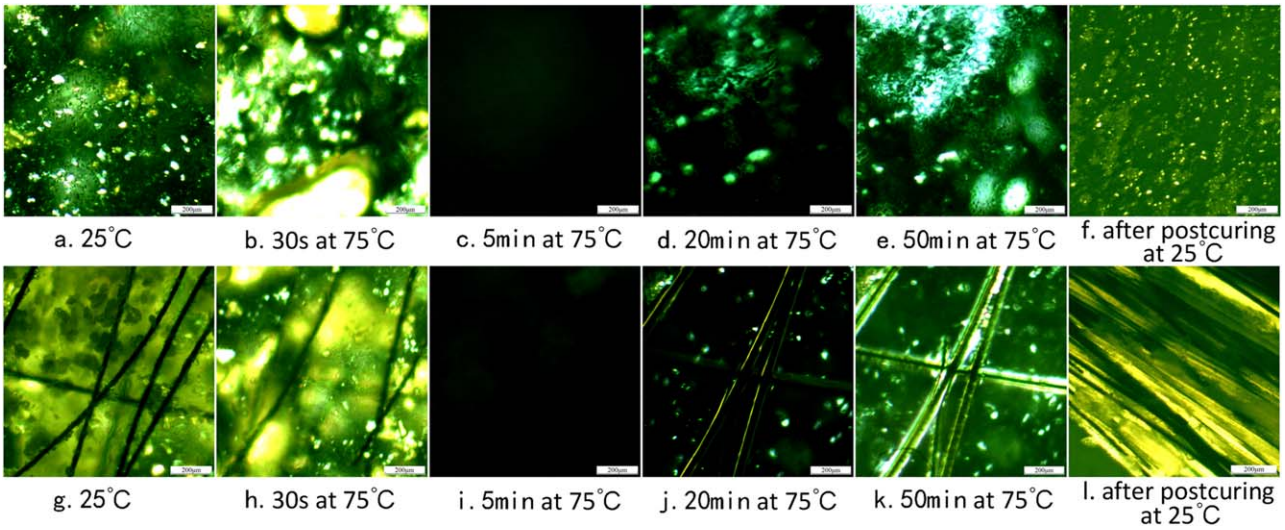

Figure 2. Polarized optical microscopic pictures of curing of LCE6/DDM (a–f) and LCE6/DDM/CF (g–l). [Color figure can be viewed in the online issue, which is available at wileyonlinelibrary.com.]

Figure 3 represents the wide angle X-ray diffraction pattern of carbon fibric, LCE6/DDM resin and LCE6/DDM/CF composite. Intense diffraction peak at 25.2° and a strong shoulder around 20.8° were observed in the direction of fiber alignment from LCE6/DDM/CF composites, while in LCE6/DDM resin only a weak peak around 20.8° was identified and even a weaker broad peak around 20.8° was seen in the transverse direction of fiber long axis.The peak at 25.2° was caused by basal plane of carbon fiber, which can be seen from intense diffraction peak of carbon fibric.

It was reported by McARDLE CB, the X-ray diffraction patterns of nematic polymers showed, in general, a typical broad peak in the region of $2\theta = 15–30°$, classically due to the average lateral distance between the neighboring chains with *d*-spacing of 3–5 Å.[18] Both LCE6/DDM resin and LCE6/DDM/CF composite illustrated a typical nematic characteristic with a broad peak around 20.8° and *d*-spacing of 4.3 Å. Even if the average lateral distance between the neighboring chains with *d*-spacing of 4.3 Å was not apparently affected in the composites, owing to be hindered by the lateral substituent. However, comparing the intense diffraction peak around 20.8° of LCE6/DDM resin and LCE6/DDM/CF composites parallel and perpendicular to fiber direction, the diffraction intensity in the direction of fiber alignment of LCE6/DDM/CF composite is stronger than the nematic network[15] diffraction intensity of LCE6/DDM, and only a weaker broad peak around 20.8° was seen in the transverse direction of fiber long axis, which proves the alignment of LCE6 network along fiber long axis. These indicate that a more regular uniaxially oriented nematic structure can be formed in the composites. It was also demonstrated by Lee et al. that LCE is more aligned along fiber long axis at lower curing temperature.[9,10] Curing of liquid crystalline epoxies includes linear chain extension at early stage, then branching, and finally crosslinking, which could have significant effects on orientation of mesogenic and structure of liquid crystalline epoxy systems. The linear chain extension, which react mainly during the curing of liquid crystalline epoxy at lower temperature, increases the orientational order, while the crosslinking, reacting mainly at higher temperature, served to lock the orientational order permanently into the network.[1,19,20] If higher temperature at early stage of curing was chosen, the linear chain extension could not catch up with the crosslinking, and the uniaxially oriented structure could not be formed. Thus, the early curing of liquid crystalline epoxy at lower temperature can more likely induce liquid crystal phase rather than isotropic state.

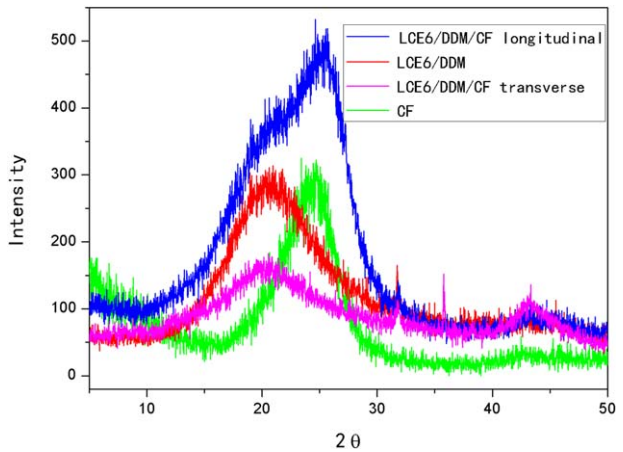

Figure 3. Wide angle X-ray diffraction measurements of LCE6/DDM/CF parallel and perpendicular to fiber direction, LCE6/DDM and CF. [Color figure can be viewed in the online issue, which is available at wileyonlinelibrary.com.]

Orientation mode of LCE6 network along long axis of carbon fiber on carbon fiber surface is shown schematically in Figure 4. LCE6 tends to be more regular uniaxially oriented nematic structure in the presence of carbon fibers curing at low temperature.

Fracture Morphology and Mechanism

The fracture surface SEM micrographs of LCE6/DDM resin and LCE6/DDM/CF composite were shown in Figure 5. The results show that both LCE6/DDM resin and LCE6/DDM/CF composite

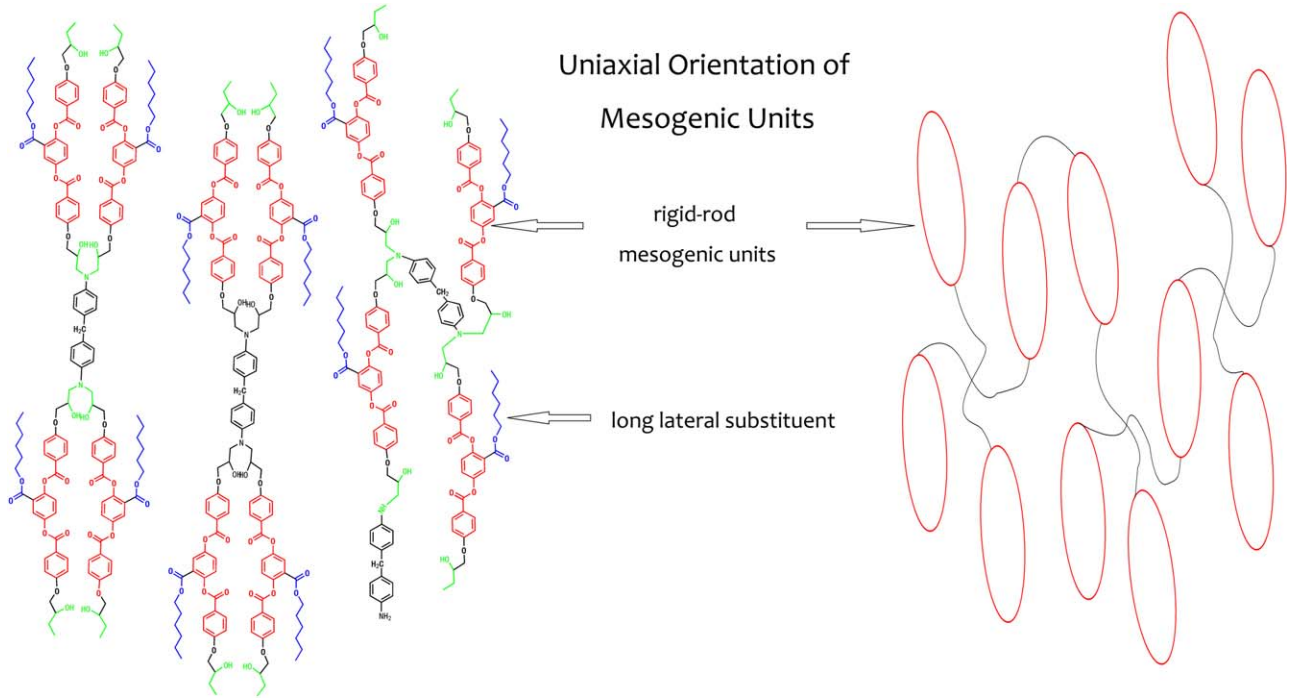

Figure 4. Uniaxial orientation of mesogenic units on carbon fiber. [Color figure can be viewed in the online issue, which is available at wileyonlinelibrary.com.]

exhibit rough and highly deformed fracture surfaces, while the composite illustrates more rough and more highly deformed fracture surfaces with LCE6 uniformly bonded to carbon fiber surface, which was observed in Figure 5(c,d).

A furrow-like deformation on the fracture surfaces of LCE6/DDM resin was observed in Figure 5(a,b), which is consistent with the work done by Sue et al.[21] It was reported by Harada et al. that liquid crystalline epoxy resin system containing mesogenic groups in the backbone moiety had high fracture toughness and the roughness of the fracture surfaces was much greater in the smectic system than in the nematic system.[22,23] Ortiz et al. reported that a liquid-crystalline phase structure, added to a stilbene-type epoxy resin system, improved the fracture toughness.[24] The alignment of LCE6 along long axis of carbon fiber (see Figures 2 and 3) can induce a more ordered nematic polydomain structure, resulting in a higher fracture toughness and LCE6 uniformly bonded to carbon fiber surface. Although the carbon fiber we used was woven carbon fabric, LCE6 was uniformly bonded to carbon fiber surface with few carbon fiber self-assembled, owing to carbon fabric being pre-impregnated by the mixed solution of LCE6/DDM and the alignment of LCE6 along long axis of carbon fiber [see Figure 2(k)]. These indicate that the toughness of the LCE6/DDM resin has been highly improved and the composite will be a potential candidate for the manufacturing of advanced composites.

Curing Degree of the Composite

FTIR spectrum of LCE6, LCE6/DDM, and LCE6/DDM/CF composite was shown in Figure 6. An absorption peak at 912 cm^{-1} is observed characteristic of the epoxy stretching in the FTIR spectrum of LCE6, while this absorption peak at 912 cm^{-1} can not be found in LCE6/DDM resin and LCE6/DDM/CF composite spectrums. These indicate both LCE6/DDM and LCE6/DDM/CF composite were completely cured and the presence of carbon fibers may not impact on the curing reaction.

Dynamic Mechanical Analysis

Figure 7 shows the loss tangent (tan δ) data of LCE6/DDM and LCE6/DDM/CF composite, from which it can be found that the T_g of LCE6/DDM/CF composite, observed at 117°C, is 5° higher than that of the LCE6/DDM resin, as is illustrated in Table I.

As is well known, T_g or α transition in DMA is the temperature at which the segments of the network begin to move. And the segmental motion of network can be affected by the chemical crosslinking, physical entanglement, and the packing density of the segments. As is shown in Figures 2 and 3, the molecule of LCE with long lateral substituent was aligned along the long axis of carbon fiber, resulting in an increased packing density of the segments. Although the alignment of LCE6 along the long axis of carbon fiber can reduce physical entanglement to some extent, the interchain interactions like hydrogen bonding can be enhanced owing to the increased packing density of the segments, making the mesogens slip and rotate not easily, even long lateral substituent may prohibit the motion of chain segments. The effect of long lateral substituent on the T_g of LCE was reported by our group in previous article.[16] As a result, the alignment of LCE6 along the long axis of carbon fiber can increase packing density of the segments and segmental motion of networks becomes difficultly. Similar results were reported elsewhere that close packed and regularly ordered LCE on

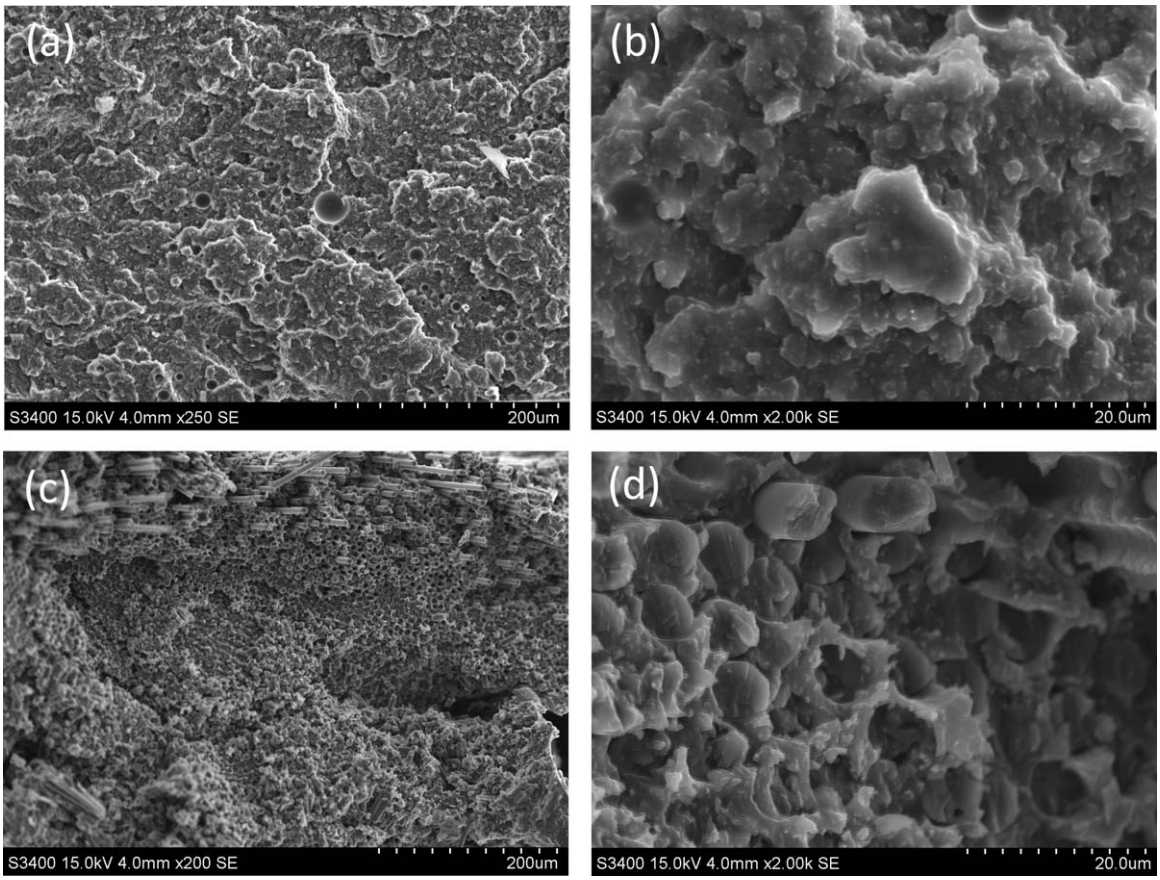

Figure 5. SEM micrographs showing fracture surface of LCE6/DDM resin [(a) low magnification, (b) high magnification] and LCE6/DDM/CF composite [(c) low magnification, (d) high magnification].

carbon fiber surface put a high barrier for chain motion of LCE in the network structure, causing the shift of T_g to higher temperatures.[9] Therefore, the higher T_g of LCE6/DDM/CF composite was attributed to the alignment of LCE6 on carbon fiber surface and the obstruction of long lateral substituent.

The dynamic storage moduli (E') and dynamic loss moduli (E'') of LCE6/DDM and LCE6/DDM/CF composite were shown in Figures 8 and 9. Broad peaks centered at about −70°C and a strong peak at about 110°C appear in the E'' curve. In correspondence with the first brosd peaks, E' is slightly reduced,

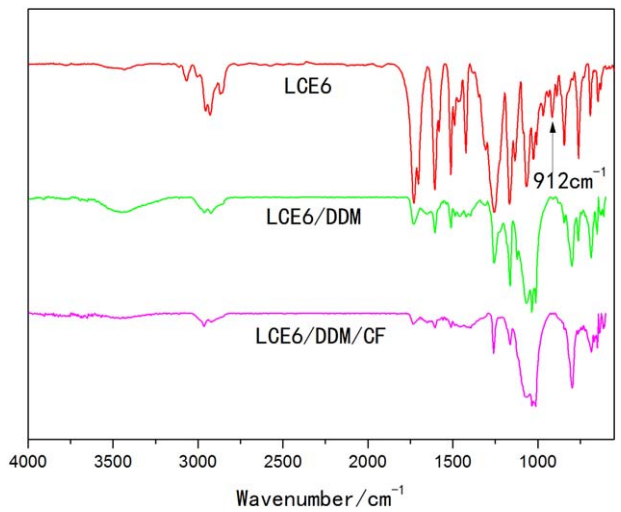

Figure 6. FTIR spectrum of LCE6, LCE6/DDM, and LCE6/DDM/CF composite. [Color figure can be viewed in the online issue, which is available at wileyonlinelibrary.com.]

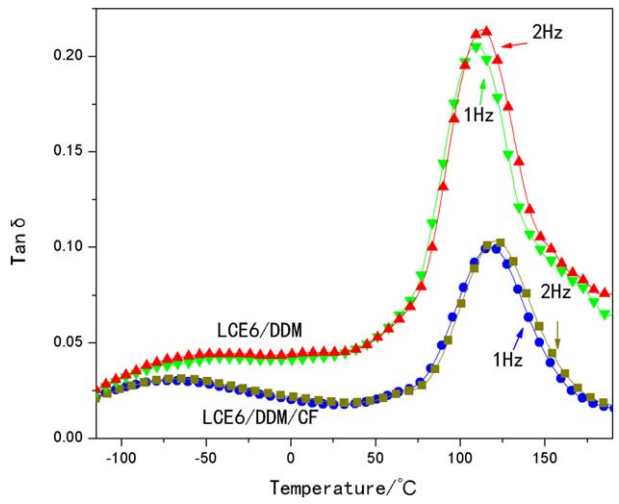

Figure 7. Loss tangent (tan δ) of LCE6/DDM and LCE6/DDM/CF composite. [Color figure can be viewed in the online issue, which is available at wileyonlinelibrary.com.]

Table I. Dynamic Mechanical Results of LCE6/DDM and LCE6/DDM/CF Composite at 2 Hz

Samples	Storage moduli (E') (GPa) 20°C	Storage moduli (E') (MPa) (T_g + 20°C)	T_g (°C)
LCE6/DDM	2.1	290	112
LCE6/DDM/CF composite	16.1	4780	117

while it drops after the peak at about 110°C for both LCE6/DDM resin and LCE6/DDM/CF composite. The strong peak at about 110°C was attributed to T_g or α transition in DMA, as was discussed above.

The broad peaks correspond to the β transition which can also be seen in the loss tangent (tan δ) data of LCE6/DDM and LCE6/DDM/CF composite (see Figure 7), originating from the small-scale motion of polymer networks, which includes the movements of side chains or pendent groups.[25] The β transition temperature show no significant difference between LCE6/DDM resin and LCE6/DDM/CF composite. It can be explained that although LCE6 was aligned along the long axis of carbon fiber, resulting in an increased packing density of the segments, the distance between mesogenic units was almost same for LCE6/DDM resin and LCE6/DDM/CF composite (It can be seen in Figure 3 that the nematic intense diffraction peaks were at around 20.8° for both LCE6/DDM resin and LCE6/DDM/CF composite).

From Figure 8 it can be found that the dynamic storage moduli (E') of the composite was extremely higher than LCE6/DDM resin. The dynamic storage moduli (E') of the composite at 20°C was 16.1 GPa, while the E' of LCE6/DDM resin at 20°C was only 2.1 GPa, as was illustrated in Table I. Although the dynamic storage moduli (E') determined with DMA in a Dual-Cantilever2x16 stress mode was not higher than E' at 20°C of

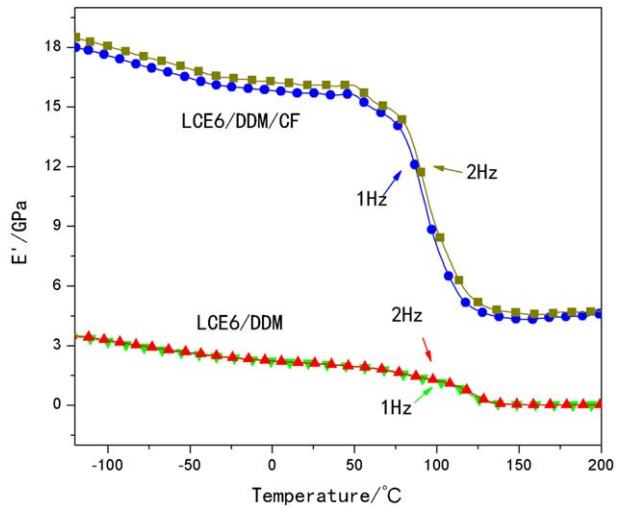

Figure 8. Dynamic storage moduli (E') of LCE6/DDM and LCE6/DDM/CF composite. [Color figure can be viewed in the online issue, which is available at wileyonlinelibrary.com.]

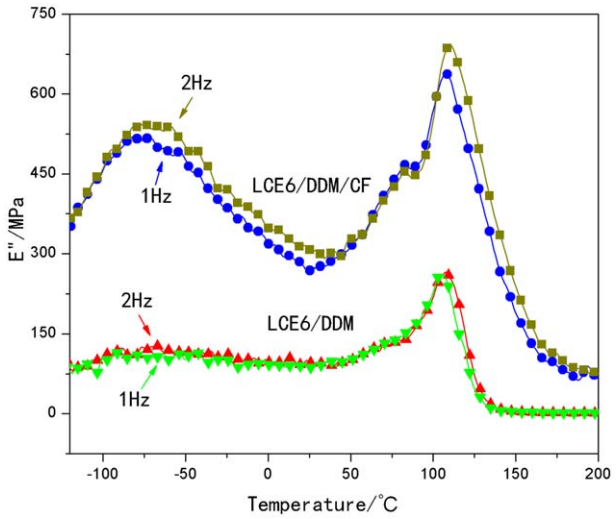

Figure 9. Dynamic loss moduli (E'') of LCE6/DDM and LCE6/DDM/CF composite. [Color figure can be viewed in the online issue, which is available at wileyonlinelibrary.com.]

the composites based on LCE and CF reported by Carfagna et al.[6] (about 20 GPa determined with DMA in tensile mode) and Lee et al.[9] (about 50 GPa determined with DMA in tensile mode), which was likely because the long lateral substituents decrease the rigidity of mesogenic core and lead mesogens orient easily in the direction of applied stress, in addition, higher toughness can be achieved owing to the long lateral substituents. Therefore, it is apparent that LCE6/DDM/CF composites possess notable mechanical properties with comparative higher dynamic storage moduli (E') and toughness, making it to be a high performance composite, which indicates that this LCE6/DDM/CF composite can be a potential candidate for advanced composites.

Thermal Degradation of LCE6/DDM/CF Composite

TGA data of LCE6/DDM was shown in Figure 10 and Table II. From TGA scans in Figure 10 it can be found that LCE6/DDM/CF composite has greater thermal stability than LCE6/DDM resin. And the 5% mass loss temperature of LCE6/DDM/CF composite at 317°C, illustrated in Table II, is higher than LCE6/DDM resin, which is at 307°C.

As known, liquid crystalline epoxides containing large rigid-rod repeating units have, in general, noticeable high-temperature properties. It was reported that the most important factor influencing the thermal stability is the molecular structure rather than phase difference.[26–29] However, the thermal stability of liquid crystalline thermosets could be affected by network structure[28] and mesogen concentration.[16,30] Although the same LCE6 and DDM were used to preprare LCE6/DDM resin and LCE6/DDM/CF composite, the molecule of LCE with long lateral substituent was cured with DDM along the long axis of carbon fiber, as is discussed at Figures 2 and 3. And the alignment of LCE6 on carbon fiber surface increases mesogen network density, which improves the thermal stability of LCE6/DDM/CF composite. From the work of Cho et al., it can be found that the cured liquid crystalline epoxy (D2A1) has higher thermal

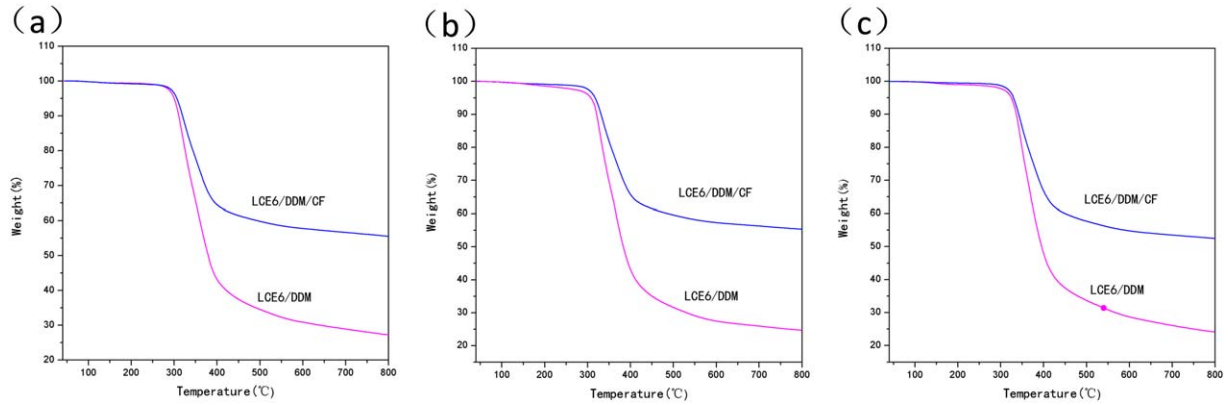

Figure 10. TGA data of LCE6/DDM and LCE6/ DDM/CF composite at different heating rate: (a) 5°C/min; (b) 10°C/min; (c) 20°C/min. [Color figure can be viewed in the online issue, which is available at wileyonlinelibrary.com.]

stability than uncured D2A1,[26] which indicates higher thermal stability is attributed to a dense mesogen network. This is why LCE6/DDM/CF composite has good high-temperature stability than LCE6/DDM resin.

Activation Energies for Degradation

A lot of work was reported about investigating the thermal stability and calculating the activation energies for decomposition of liquid crystalline polymers.[11,26,27,31–35] In this work, the activation energies for decomposition of LCE/DDM resin and LCE/DDM/CF composites under nitrogen atmosphere were calculated according to Kissinger[36] and Flynn–Wall–Ozawa method.[37,38]

The Kissinger and Flynn–Wall–Ozawa method can be expressed respectively as follows

$$\mathrm{Ln}\ \left(\beta/T^2\right)=A-E_d/RT \quad (1)$$

$$\mathrm{Ln}\ \beta=C-E_d/RT \quad (2)$$

where A and C are constants at conversion α, β is the heating rate, R is the gas constant, E_d is the activation energy, and T is the absolute temperature at conversion α and heating rate β. And conversion α mentioned above is the ratio of actual weight loss to total weight loss.

Figure 11 shows the Kissinger and Flynn–Wall–Ozawa plots for LCE6/DDM resin at different conversions, while the Kissinger and Flynn–Wall–Ozawa plots for LCE6/DDM/CF composite at different conversions are shown in Figure 12. And the decomposition activation energies of LCE6/DDM resin and LCE6/DDM/CF composite at different conversions are obtained and listed in Table III. Parallel plots were shown in Figures 11 and 12, which indicates almost constant activation energies for both the LCE6/DDM resin and LCE6/DDM/CF composite. While the LCE6/DDM/CF composite shows, at conversions from 0.1 to 0.4, higher activation energies than LCE6/DDM resin, and no significant difference at conversions above 0.5, comparing the activation energies in Table III.

It was reported by Giamberini et al. that the decomposition mechanisms depend on the network microstructures and activation energies for the LC sample are significantly higher than those for the ISO sample.[11] As is discussed above, owing to the presence of carbon fiber, LCE6 was aligned along long axis of carbon fiber, resulting in a dense mesogen network. After curing of the composites, a lot of hydroxy appear in the composites (see Figure 4). And a more close packed mesogen network can enhance intermolecular interactions like hydrogen bond, which hinders complete degradation in a single bond cleavage. And also the dense mesogen network keeps molecular chains close to each other, thus allowing recombination of the free radicals.[11,28,39] Therefore, at degradation of the initial part, LCE6/DDM/CF composite shows higher activation energies than LCE6/DDM resin because of the alignment of LCE6 on carbon fiber surface. Once this orientation of LCE6 on carbon surface is lost (extent of conversion greater than 0.5), the energy appears no significant difference, as the alignment structure caused by carbon fiber is broken, and the E_a values of the two systems converge.

CONCLUSIONS

A high performance composites based on carbon fiber and liquid crystalline epoxy with lateral substituent was prepared and investigated in this article. Polarized optical microscopy and wide angle X-ray diffraction measurements indicate that liquid

Table II. Results of Thermal Degradation of LCE6/DDM and LCE6/DDM/CF Composite Measured by TGA in Nitrogen at 5, 10, 20°C/min Heating Rate

	LCE6/DDM			LCE6/DDM/CF composite		
Samples	5°C/min	10°C/min	20°C/min	5°C/min	10°C/min	20°C/min
5% mass loss temperature (°C)	300	307	324	306	317	329
Residual weight (%)	27.3	24.7	24.1	55.5	55.3	52.5

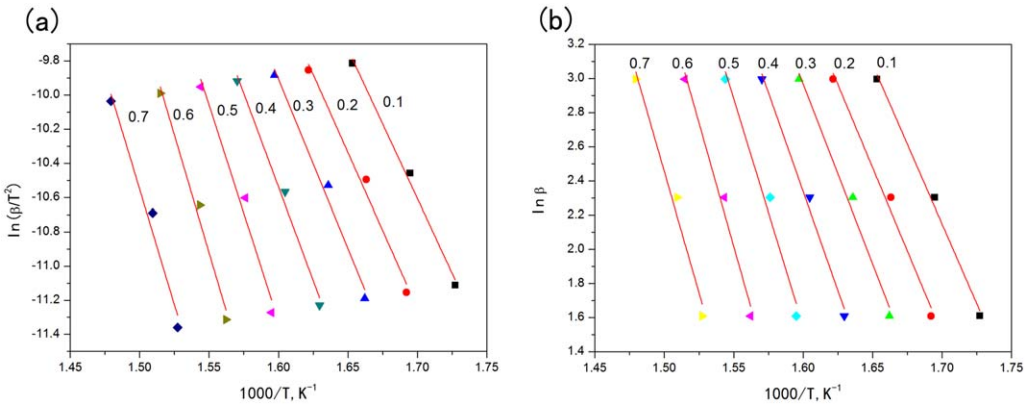

Figure 11. Kissinger (a) and Flynn–Wall–Ozawa (b) plots for LCE6/DDM resin at different conversions. [Color figure can be viewed in the online issue, which is available at wileyonlinelibrary.com.]

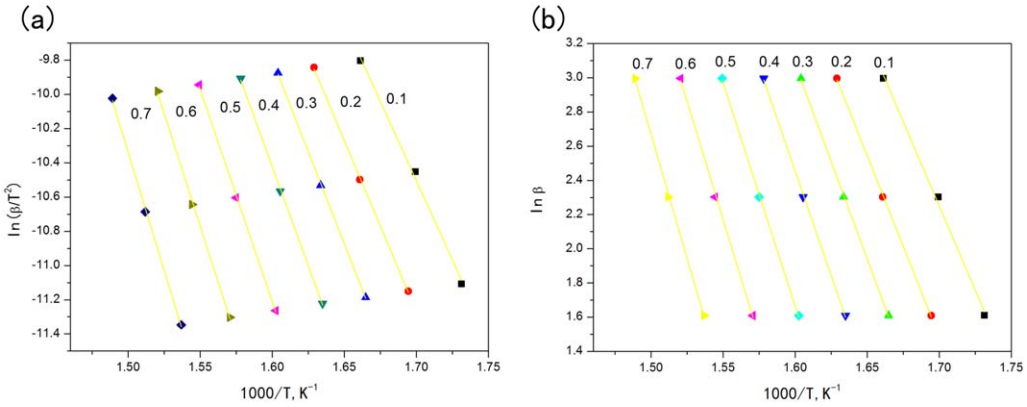

Figure 12. Kissinger (a) and Flynn–Wall–Ozawa (b) plots for LCE6/DDM/CF composite at different conversions. [Color figure can be viewed in the online issue, which is available at wileyonlinelibrary.com.]

crystalline epoxy with lateral substituent was aligned along long axis of carbon fiber. The fracture surface SEM micrographs show the composite illustrates more rough and more highly deformed fracture surfaces with a good interfacial adhesion between carbon fibers and resin. Thermogravimetric (TGA) analysis shows, in general, a higher thermal stability and higher decomposition activation energies of the composite at degradation of the initial part, which indicates that the thermal resistance can be improved by the alignment of LCE6 on carbon fiber surface. The dynamic mechanical analysis shows that the composites possess a higher T_g and extremely higher dynamic storage moduli, which indicates that this LCE6/DDM/CF composite can be a high performance composite, a potential candidate for advanced composites and can be applied into aerospace structural materials.

Table III. Results of Activation Energy of LCE6/DDM and LCE6/DDM/CF Composite

	Activation energy (kJ/mol)			
	LCE6/DDM		LCE6/DDM/CF	
Conversion	Kissinger	Ozawa	Kissinger	Ozawa
0.1	145	155	154	164
0.2	151	162	166	176
0.3	164	175	179	189
0.4	182	192	192	203
0.5	210	221	206	217
0.6	229	240	218	230
0.7	224	238	229	241

ACKNOWLEDGMENTS

This research is financially supported by the National Natural Science Foundation of China (20974121).

REFERENCES

1. Barclay, G. G.; Ober, C. K. *Prog. Polym. Sci.* **1993**, *18*, 899.
2. Carfagna, C.; Amendola, E.; Giamberini, M. *Compos. Struct.* **1994**, *27*, 37.
3. Stenzenberger, H. D. *Compos. Struct.* **1993**, *24*, 219.

4. Frank, E.; Hermanutz, F.; Buchmeiser, M. R. *Macromol. Mater. Eng.* **2012**, *297*, 493.
5. Mally, T. S.; Johnston, A. L.; Chann, M.; Walker, R. H.; Keller, M. W. *Compos. Struct.* **2013**, *100*, 542.
6. Carfagna, C.; Meo, G.; Nicolais, L.; Giamberini, M.; Priola, A.; Malucelli, G. *Macromol. Chem. Physic.* **2000**, *201*, 2639.
7. Carfagna, C.; Acierno, D.; Di Palma, V.; Amendola, E.; Giamberini, M. *Macromol. Chem. Physic.* **2000**, *201*, 2631.
8. Carfagna, C. *Abstr. Pap. Am. Chem. S.* **2000**, *219*, U503.
9. Lee, J. Y.; Jang, J. *Polym. Bull.* **2007**, *59*, 261.
10. Lee, J. Y. *J. Appl. Polym. Sci.* **2006**, *102*, 684.
11. Giamberini, M.; Malucelli, G.; Ambrogi, V.; Capitani, D.; Cerruti, P. *Polym. Int.* **2010**, *59*, 1415.
12. Mallon, J. J.; Adams, P. M. *Mol. Cryst. Liq. Cryst.* **1992**, *213*, 173.
13. Adams, P. M.; Mallon, J. J. *Mol. Cryst. Liq. Cryst.* **1991**, *208*, 65.
14. Zheng, Y. Q.; Ren, S. P.; Ling, Y. D.; Lu, M. G. *Mol. Cryst. Liq. Cryst.* **2006**, *452*, 3.
15. Zheng, Y.; Shen, M.; Lu, M.; Ren, S. *Euro. Polym. J.* **2006**, *42*, 1735.
16. Zheng, Y.; Lu, M.; Ren, S.; Hang, L.; Lan, Y. *J. Polym. Sci. Part B: Polym. Phys.* **2007**, *45*, 2835.
17. Liang, L.; Ren, S.; Zheng, Y.; Lan, Y.; Lu, M. *Polym. J.* **2007**, *39*, 961.
18. Mcardle, C.B. Side Chain Liquid Crystal Polymers, Chap 6, Chapman and Hall: New York, NY; **1989**.
19. Shiota, A.; Ober, C. K. *Prog. Polym. Sci.* **1997**, *22*, 975.
20. Giamberini, M.; Amendola, E.; Carfagna, C. *Mol. Cryst. Liq. Crys. A* **1995**, *266*, 9.
21. Sue, H. J.; Earls, J. D.; Hefner, R. E. *J. Mater. Sci.* **1997**, *32*, 4031.
22. Harada, M.; Aoyama, K.; Ochi, M. *J. Polym. Sci. Part B: Polym. Phys.* **2004**, *42*, 4044.
23. Harada, M.; Okamoto, N.; Ochi, M. *J. Polym. Sci. Part B: Polym. Phys.* **2010**, *48*, 2337.
24. Ortiz, C.; Kim, R.; Rodighiero, E.; Ober, C. K.; Kramer, E. J. *Macromolecules* **1998**, *31*, 4074.
25. Tan, C. B.; Sun, H.; Fung, B. M.; Grady, B. P. *Macromolecules* **2000**, *33*, 6249.
26. Cho, S. H.; Lee, J. Y.; Douglas, E. P.; Lee, J. Y. *High Perform. Polym.* **2006**, *18*, 83.
27. Lu, M. G.; Shim, M. J.; Kim, S. W. *J. Appl. Polym. Sci.* **2000**, *75*, 1514.
28. Gavrin, A. J.; Curts, C. L.; Douglas, E. P. *J. Polym. Sci. Part A: Polym. Chem.* **1999**, *37*, 4184.
29. Pramoda, K. P.; Chung, T. S.; Liu, S. L.; Oikawa, H.; Yamaguchi, A. *Polym. Degrad. Stab.* **2000**, *67*, 365.
30. Duann, Y. F.; Liu, T. M.; Cheng, K. C.; Su, W. F. *Polym. Degrad. Stab.* **2004**, *84*, 305.
31. Fache, B.; Gallot, B.; Gelin, M. P.; Milano, J. C.; Quang Trung, P. *J. Appl. Polym. Sci.* **2013**, *127*, 3798.
32. Li, X. G. *Polym. Degrad. Stab.* **1999**, *65*, 473.
33. Li, X. G.; Huang, M. R.; Guan, G. H.; Sun, T. *Polym. Degrad. Stab.* **1999**, *65*, 463.
34. Vincent, L.; Mija, A.; Sbiffazzuoli, N. *Polym. Degrad. Stab.* **2007**, *92*, 2051.
35. Liu, Y.-L.; Cai, Z.-Q.; Wen, X.; Pi, P.; Zheng, D.; Cheng, J.; Yang, Z. *Thermochim Acta* **2011**, *513*, 88.
36. Kissinger, H. E. *Anal. Chem.* **1957**, *29*, 1702.
37. Ozawa, T. *Bull. Chem. Soc. Jpn.* **1965**, *38*, 1881.
38. Flynn, J. H.; Wall, L. A. *J. Polym. Sci. Part B: Polym. Lett.* **1966**, *4*, 323.
39. Arnold, C. *Macromol. Rev. Part D-J. Polym. Sci.* **1979**, *14*, 265.